Extrasolar planet detection through spatially resolved observations

Meshkat, T.R.

Chapter 5

Discovery of a Low-Mass Companion to the F7V star HD 984

We report the discovery of a low-mass companion to the nearby ($d = 47$ pc) F7V star HD 984. The companion is detected $0\farcs19$ away from its host star in the L' band with the Apodizing Phase Plate on NaCo/VLT and was recovered by L'-band non-coronagraphic imaging data taken a few days later. We confirm the companion is co-moving with the star with SINFONI integral field spectrograph $H+K$ data. We present the first published data obtained with SINFONI in pupil-tracking mode. While HD 984 has been argued to be a kinematic member of the 30 Myr-old Columba group, and its HR diagram position is not altogether inconsistent with being a ZAMS star of this age, we independently estimate a main sequence isochronal age of $2.0^{+2.1}_{-1.8}$ Gyr which does not rely on this kinematic association. The mass of directly imaged companions are usually inferred from theoretical evolutionary tracks, which are highly dependent on the age of the star. Based on the age extrema, we demonstrate that with our photometric data alone, the companion's mass is highly uncertain: between 33 and 120 M_{Jup} (0.03-0.11 $M_\odot$) using the COND evolutionary models. We compare the companion's SINFONI spectrum with field dwarf spectra to break this degeneracy. Based on the slope and shape of the spectrum in the H-band, we conclude that the companion is an M6.0 ± 0.5 dwarf. The age of the system remains unconstrained, as M dwarfs are poorly fit on low-mass evolutionary tracks. This discovery emphasizes the importance of obtaining a spectrum to spectral type companions around F-stars.

T. Meshkat, M. Bonnefoy, E. E. Mamajek, S. P. Quanz, G. Chauvin, M. A. Kenworthy, J. Rameau, M. R. Meyer, A.-M. Lagrange, J. Lannier, P. Delorme
Submitted to *Monthly Notices of the Royal Astronomical Society*

5.1 Introduction

Young stars are the primary targets of exoplanet imaging surveys because associated planets are warm and therefore bright in the infrared. A handful of brown dwarfs and low-mass stellar companions have been found in these surveys (PZ Tel B; Biller et al. 2010, CD-35 2722 B; Wahhaj et al. 2011, HD 1160 B,C; Nielsen et al. 2012). Masses of directly imaged companions are estimated from the companion's luminosity and theoretical evolutionary models, which are very sensitive to the age and distance of the host star.

The companion mass-ratio distribution (CMRD) quantifies the mass ratio of a binary system (Reggiani & Meyer 2013). Based on observational data, the initial mass function (IMF) for brown dwarfs and very-low-mass-stars (0.08-0.2$M_{\odot}$) likely differs from stars (Thies et al. 2015). The primary formation mechanisms for these low-mass companions, including fragmentation and capture, is still under debate, making each new discovered low-mass companion an important test case for the theoretical formation mechanisms of low-mass companion. The orbital motion of the companion around the primary star, measured as a small arc on the sky, can be used to find orbital solutions (Pearce et al. 2015). Some orbital properties, such as eccentricity, can be constrained with only two measurements (Biller et al. 2010). Additionally, with multiple epoch astrometric measurements from direct imaging and radial velocity data, the dynamical mass of a companion can be measured. This acts as an important comparison with the inferred companion masses from theoretical evolutionary models (Bonnefoy et al. 2009; Dupuy et al. 2015; Close et al. 2007).

We report the detection of a companion around the F7V star HD 984 (HIP 1134). This star has been part of many imaging surveys searching for planets (Brandt et al. 2014; Rameau et al. 2013a) due to its proximity, brightness ($d = 47.1 \pm 1.4$ pc; V = 7.3; ESA 1997; van Leeuwen 2007), and proposed youth (30 Myr, Zuckerman et al. 2011). However, no comoving companions have yet been reported. Ground-based sub-mm and *Spitzer* infrared photometry of HD 984 have not detected any evidence of a dusty debris disk (Mamajek et al. 2004; Carpenter et al. 2009; Ballering et al. 2013).

In Section 6.2 we describe our coronagraphic and non-coronagraphic observations with NaCo on the VLT, and our SINFONI/VLT integral field spectrographic data. In Section 5.3 we measure the companion's photometry and astrometry. In Section 5.4 we discuss previous age estimates of HD 984, and estimate its main sequence isochronal age. In Section 5.5 we estimate the mass of the companion based on evolutionary models and spectral analysis. We conclude in Section 5.6.

5.2 Observations

5.2.1 NaCo/VLT

Observations of HD 984 were taken on UT 2012 July 18 and 20 (089.C-0617(A), PI: Sascha Quanz) at the Very Large Telescope (VLT)/UT4 with NaCo (Lenzen et al. 2003; Rousset et al. 2003). The Apodized Phase Plate coronagraph (APP;

Kenworthy et al. 2010; Quanz et al. 2010) was used for diffraction suppression thus increasing the chances of detecting a companion very close to the target star. Data were obtained with the L27 camera, in the L'-band filter ($\lambda = 3.80\mu$m and $\Delta\lambda = 0.62\mu$m). The visible wavefront sensor was used with HD 984 as the natural guide star. We observed in pupil tracking mode (Kasper et al. 2009) for Angular Differential Imaging (ADI; Marois et al. 2006). We intentionally saturated the PSF core to increase the signal-to-noise from potential companions in each exposure. Unsaturated data were also obtained to calibrate photometry relative to the central star.

The APP suppresses diffraction over a 180° wedge on one side of the target star. Excess scattered light is increased on the other side of the target that is not used in the data analysis. Two datasets were obtained with different initial position angles (P.A.) for full 360° coverage around the target star. The field rotation was 47°.4 in the first hemisphere and 42°.5 in the second hemisphere.

Direct imaging observations of HD 984 were obtained on VLT/NaCo on UT 2012 July 20 (089.C-0149(A), PI: Julien Rameau). The data were taken with the L27 camera on NaCo in ADI pupil tracking mode. Both the saturated and unsaturated data were imaged in L'-band with the same exposure time, but in the unsaturated images a neutral density filter (ND_LONG) was used. The field rotation was 41°.3 in the direct imaging data. All datasets were obtained in cube mode. Each APP cube contains 120 frames, with an integration time of 0.5 s per frame. The total integration time in the APP was 60 min in hemisphere 1 (60 cubes) and 66 min in hemisphere 2 (66 cubes). Unsaturated APP exposures were 0.056 s per frame (222 frames in 12 cubes), with a total time on target of 150 seconds. The direct imaging cubes contain 100 frames, with 0.2 s per frame, with a total integration time of 48 min for the saturated data and 202 seconds for the unsaturated data.

A dither pattern on the detector was used to subtract sky background and detector systematics from both datasets, as detailed in Kenworthy et al. (2013). Data cubes are subtracted from each other, centroided and averaged over. Optimized principal component analysis (PCA) is run on both of the APP hemispheres and direct imaging data independently, following Meshkat et al. (2014). Six principal components are used to model the stellar PSF, which results in the highest signal-to-noise detection of the companion. PCA processed frames are derotated and averaged to generate the final image with North facing up.

5.2.2 SINFONI/VLT

Data were obtained on HD 984 with the AO-fed integral field spectrograph SINFONI (Eisenhauer et al. 2003; Bonnet et al. 2004) at the VLT on UT 2014 September 9 (093.C-0626, PI: G. Chauvin) in $\sim 0''.5$ seeing. The $H + K$ grating was used, which has a resolution of ~1500. The spatial sampling was 12.5 mas×25 mas (in the horizontal and vertical directions, respectively) resulting in a field of view of $0''.8 \times 0''.8$. We obtained 42 raw cubes of the target, each consisting of 10×4s coadded exposures. Similar to the NaCo observations, data were obtained in pupil tracking (PT) mode (Hau et al. in prep). The companion rotated 49.26° around

the center of the field of view during our 28 min integration.

The instrument pipeline version 2.5.2 [1] was used to correct the raw science frames from hot and non-linear pixels, detector gain, and distortion. Final cubes were reconstructed from the resulting frames, associated wavelength map, and slitlet positions. Data cubes were corrected for OH lines and background emission using a dedicated algorithm (Davies 2007) implemented in the pipeline.

The wavelength-dependent drift in the star position, caused by the atmospheric refraction, was registered (modeled by a 3rd order polynomial) and corrected. We took the mean of the parallactic angle values at the beginning and end of a given exposure, which is stored in the cube file headers. We processed the cubes with the classical-ADI (CADI) algorithm (Marois et al. 2006) to suppress the stellar flux independently at each wavelength (2172 independent spectral resolution elements).

Data were corrected for telluric absorption lines using the observations of an A3V standard star (HD 2811) obtained close in time to HD 984 and at a comparable airmass. The resulting spectrum of HD 984 was flux-calibrated using the 2MASS H-band magnitude of the star (Cutri et al. 2003) and a spectrum of Vega.

5.3 Photometry and Astrometry of HD 984 B

5.3.1 NaCo/VLT

The companion was clearly detected very close to the star (Figure 5.1, APP hemisphere 1 on top-left and direct imaging on top-right). The companion detection was confirmed using the *Pynpoint* pipeline (Amara & Quanz 2012) and the IPAG-ADI pipeline (Chauvin et al. 2012). The detection was robust against changing the number of principal components used in the stellar PSF model.

We used artificial negative companions to determine the astrometry and photometry of the companion (following Meshkat et al. 2015). The unsaturated stellar PSF was used to generate artificial companions in the APP and direct imaging data. A scaling factor of 0.018 was applied to the direct imaging unsaturated data to account for the attenuation from the neutral density filter. We injected artificial negative companions into the data near the expected position of the companion in steps of 0.1 pixels. The artificial companion contrast was varied from 5.0 to 7.0 in steps of 0.01 mag. The chi-squared minimization over the λ/D patch at the location of the artificial negative companion yielded the following results.

Based on this analysis, the companion contrast in the APP data is best approximated as $\Delta L' = 6.0 \pm 0.2$ mag ($L' = 12.0 \pm 0.2$mag). The angular separation of the companion is $0\farcs19 \pm 0.02$, which corresponds to a projected separation of 9.0±1.0 AU for the stellar distance of 47.1 ± 1.4 pc from van Leeuwen (2007). The position angle (P.A.) of the companion is $108\fdg8 \pm 3\fdg0$. The error in the measurements is due to the range in artificial companions which successfully subtract the companion signal.

The companion contrast in the direct imaging data is $\Delta L' = 5.9 \pm 0.3$ mag at $0\farcs208 \pm 0.023$ (9.8 ± 1.1 AU). The P.A. of the companion is $108\fdg9 \pm 3\fdg1$ corrected

[1] http://www.eso.org/sci/software/pipelines/sinfoni/sinfoni-pipe-recipes.html

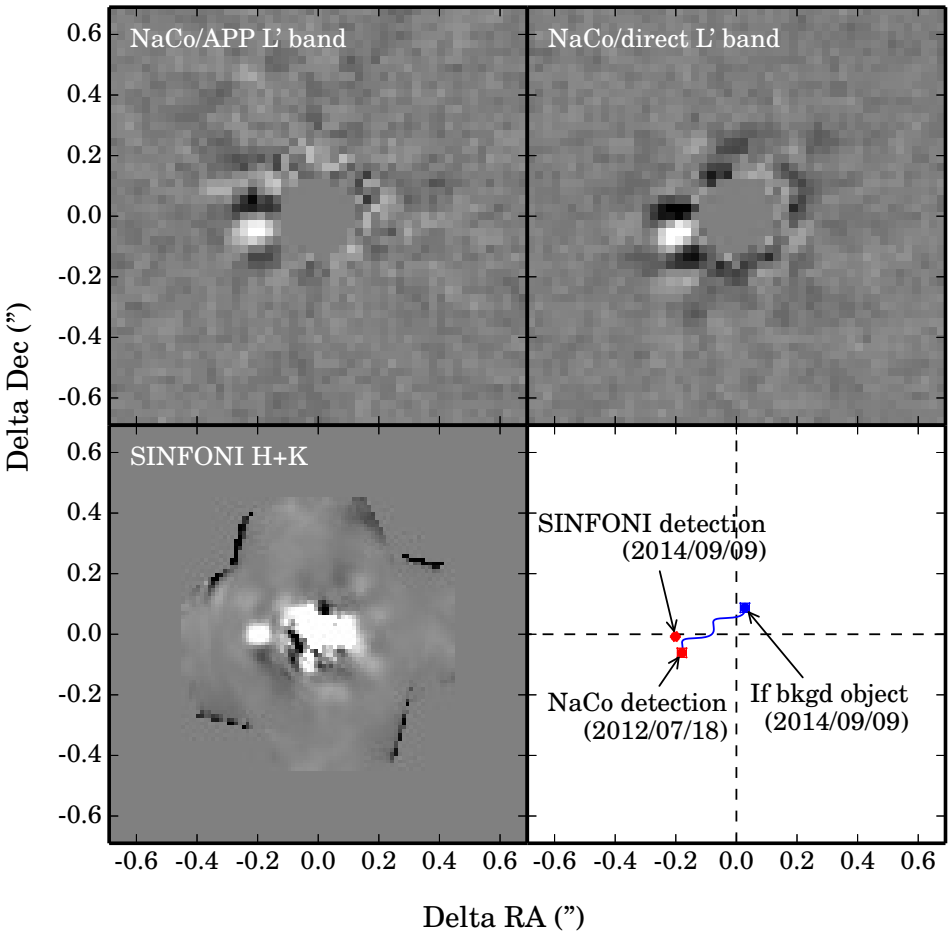

Figure 5.1 Top-left: Final PCA processed image of HD 984 APP hemisphere 1 data with North facing up. Twenty principal components were used to model the stellar PSF in this image. Top-right: Final PCA processed image of HD 984 from direct imaging data with North facing up. Six principal components were used to model the stellar PSF. Bottom-left: Collapsed $H + K$ SINFONI IFS data cubes processed with CADI, with North facing up. All three images are displayed in the same color scale. Bottom-right: The position of the companion is plotted as red points for both the VLT/NaCo dataset epoch (UT 2012 July 18) and the VLT/SINFONI epoch (UT 2014 September 9). The blue point is the position of the companion if it were a background source at the time of the VLT/SINFONI dataset epoch (UT 2014 September 9). Error bars are included for all points.

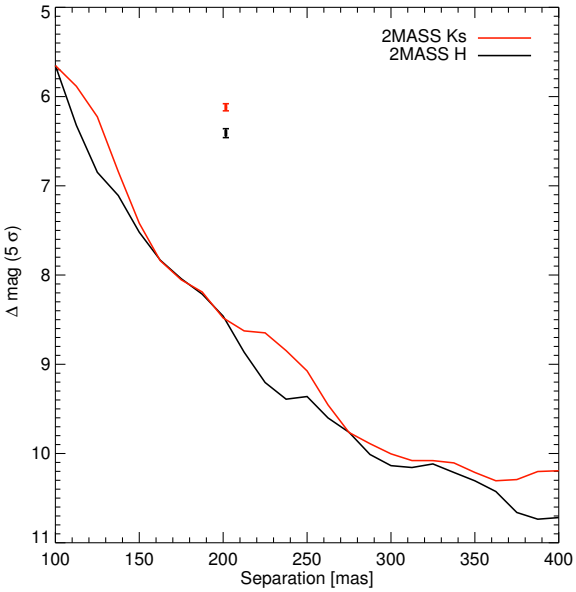

Figure 5.2 Contrast curves for the SINFONI HD 984 H (black curve) and Ks (red curve) data, for CADI processing. The companion detection is shown as a point with error bars in H (black) and Ks (red), respectively.

to true North orientation, calibrated using θ Ori, observed at the same epoch with the same mode. The θ Ori stars TCC058, 057, 054, 034, and 026 were used to determine the true North 0.41±0.07° with a plate scale of 27.11±-0.02 mas (Rameau et al. 2013a). The astrometry and photometry of the companion is in good agreement between the two datasets. Since the two datasets were only taken two days apart, we do not consider them separate epochs, but rather a confirmation that this companion is not an artifact.

5.3.2 SINFONI

The companion was detected in H+K band IFS SINFONI data (Figure 5.1 bottom-left). These data are the first published results demonstrating the capabilities of the SINFONI instrument in PT mode. The parallactic angle associated with each of the 43 data cubes was estimated by taking the mean of the parallactic angle at the beginning and the end of an exposure. We applied an additional clockwise rotation of 210.92° to the frames at the ADI reduction step to properly realign the field of view to the North. True North was estimated using GQ Lup SINFONI observations on UT 2013 August 24, which were calibrated with NaCo observations of the same source on UT 2012 March 3, assuming orbital motion is negligible between the epochs (following the formulae described in the Appendix).

The companion is detected in all of our ADI analyses. We discovered that subtracting the stellar halo of the data cubes collapsed in wavelength followed by

a realignment of the frame to the North also allowed detection of the companion. Unlike ADI processing, this allows for a measurement of the position of the companion without the biases associated with the self-subtraction of the companion PSF (Bonnefoy et al. 2011). We selected 10 frames corresponding to the first 10 cubes of the PT sequence and median-combined them after realigning to true North. This provided a good removal of residual speckles from the stellar halo. We found that HD 984 B lies at a PA=$92.2 \pm 0.5°$ and a separation $\rho = 201.6 \pm 0.4$ mas. The error considers uncertainties in our fitting function as well as true North. We also make the assumption that the instrument absolute orientation on sky did not vary between our UT 2014 September 9 observations and the True North calibration (UT 2013 August 24) with GQ Lup. The separation assumes a plate scale of 12.5 mas/pixel reported in the instrument user manual. The plate scale at the time of HD 984 observations could not be measured.

HD 984 is a relatively high proper motion star, with $\mu_{\alpha*}$, μ_δ = 102.79 ± 0.78, -66.36 ± 0.36 mas yr^{-1} (van Leeuwen 2007). If the companion were a background source, it should be due North of HD 984 and at a projected separation of $< 0\farcs1$ in the SINFONI data (Figure 5.1, bottom-right). We estimate that the companion is very unlikely to be a stationary background source, with an estimated χ^2 <1E-6 based on the two epoch companion detections, stellar proper motion, distance estimates, and the astrometric error on the SINFONI dataset (which is dependent on the plate scale). The new P.A. of the companion is consistent with Keplerian orbital motion. Based on the astrometry of the companion, we confirm it is bound to the star and not a background object.

The companion flux was integrated in a 6 pixel wide circular aperture in the processed CADI cubes to generate the spectrum. We applied the same procedure to HD 984. We corrected for flux losses in the companion's spectrum (caused by the image processing algorithms) by adding artificial sources. We used the unsaturated primary star itself to scale and inject artificial sources in the data. Artificial sources were added in each wavelength at the same projected separation as the companion, but with a P.A. difference of -90, +90, and +180°. The resulting spectrum was corrected for the telluric lines using the primary spectrum. We obtained the final flux-calibrated spectrum of the companion by multiplying the flux ratio between the system components and the flux-calibrated spectrum of the star. Based on the flux ratio between HD 984 and B in H and Ks-band, we estimate H_{2MASS} = 12.58 ± 0.05 mag and Ks_{2MASS} = 12.19 ± 0.04 mag for the companion. The spectrum of the companion is analyzed in Section 5.5.

Figure 5.2 shows contrast curves comparing the sensitivity to point sources in the data processed with the CADI algorithm in H and Ks-band. The contrast curve was generated following Chauvin et al. (2015). We injected fake planets every 10 pixels radially at P.A.s of 0, 120, and 240° between 125 and 375 mas, in order to correct for flux losses. The fake planets are created by scaling the flux of the primary star. We created a pixel-to-pixel noise map by sliding a box of 5×5 pixels from the star to the limit of the SINFONI field of view. The 5σ detection limit is found by dividing the pixel-to-pixel noise map by the flux loss, taking into account the relative calibration between the fake planet and the primary star.

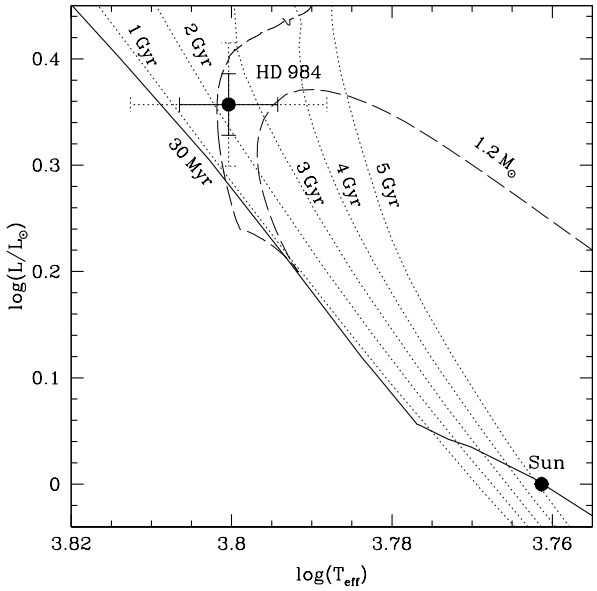

Figure 5.3 HR diagram position of HD 984 and the Sun, with isochrones and evolutionary tracks from Bressan et al. (2012) overlaid (z = 0.017), with 1σ solid line and 2σ dotted line error bars. The solid line is a 30 Myr isochrone corresponding to the purported age of the Columba group. Dotted lines are isochrones with ages of 1, 2, 3, 4, 5 Gyr. The dashed line is a 1.20 ± 0.06 (95%CL) $M_\odot$ track.

5.4 Age of HD 984

5.4.1 Previous Age Estimates

Zuckerman et al. (2011) and Malo et al. (2013) consider HD 984 to be a member of the Columba group with an age of 30 Myr (Torres et al. 2008). However, isochronal ages of <0.48 Gyr (68%CL; Takeda et al. 2007), $1.2^{+0.7}_{-0.9}$ Gyr (Valenti & Fischer 2005), and $3.1^{+1.0}_{-1.6}$ Gyr (Holmberg et al. 2009) have been estimated. HD 984 is notably chromospherically and coronally active. Wright et al. (2004) estimate an age of 0.49 Gyr based on chromospheric activity, however the star has mass ~1.2 $M_\odot$, so activity-age or gyrochronology relations for Sun-like stars are inapplicable (e.g. Mamajek & Hillenbrand 2008). Malo et al. (2013) have convincingly shown that HD 984 is consistent with comoving with Columba. However, there remains the possibility that HD 984 could be a kinematic interloper.

5.4.2 Stellar Parameters and Isochronal Age

HD 984 is a V = 7.32 mag (ESA 1997) F7V star (Houk & Swift 1999) at distance 47.1 ± 1.4 pc (van Leeuwen 2007, $\varpi = 21.21 \pm 0.64$ mas). It is not listed in latest

Property	HD 984		HD 984 B
Distance (pc)[a]		47.1 ± 1.4	
Age (Myr)[b]		$2.0^{+2.1}_{-1.8}$	
A_V [c]		0.02 ± 0.02	
$T_{\rm eff}$	6315 ± 89		2777^{+127}_{-130} [d]
			2900 ± 200 [e]
Spectral type	F7V		M6.0 ± 0.5
$\log(L/L_\odot)$	0.36 ± 0.03		-2.815±0.024
Separation (")		201.6 ± 0.4	
P.A.(°)		92.2 ± 0.5	
H	6.170 ± 0.023		12.58 ± 0.05
Ks	6.073 ± 0.038		12.19 ± 0.04
L'	6.0 ± 0.1		12.0 ± 0.2

[a] *Hipparcos* catalog (van Leeuwen 2007).
[b] This work.
[c] Schlegel et al. (1998) and Reis et al. (2011).
[d] Based on the spectral type conversion scale of Stephens et al. (2009).
[e] Based on BT-COND and GAIA synthetic spectra.

Table 5.1 System properties

version[2] of the Washington Double Star catalog (Mason et al. 2001). Considering the star's proximity, and the reddening maps of Schlegel et al. (1998) and Reis et al. (2011), we adopt $A_V = 0.02 \pm 0.02$ mag, $A_{Ks} = 0.002 \pm 0.002$ mag.

Numerous estimates of the effective temperature have been reported (e.g. Valenti & Fischer 2005; Masana et al. 2006; Schröder et al. 2009; Casagrande et al. 2011). We adopt the recent value from Casagrande et al. (2011) (6315 ± 89 K). From fitting the optical-infrared photometry to the dwarf color sequences from Pecaut & Mamajek (2013), and taking into account the previously mentioned extinction constraints, we derive an apparent bolometric magnitude of HD 984 to be $m_{bol} = 7.23 \pm 0.03$ and bolometric flux of 32.7 ± 0.9 pW m^{-2}. Employing the van Leeuwen (2007) parallax, this bolometric flux translates to a luminosity of $\log(L/L_\odot) = 0.36 \pm 0.03$ dex. Adopting the Casagrande et al. (2011) $T_{\rm eff}$, this is consistent with a stellar radius of 1.26 ± 0.06 $R_\odot$.

The HR diagram position of HD 984 is plotted in Figure 5.3 along with isochrones from Bressan et al. (2012) (for Z = 0.017). HD 984 is a main sequence star, and any derived isochronal age will have large uncertainties. Simulating the HR diagram position and interpolating their ages and masses, the isochronal ages are consistent with $2.0^{+2.1}_{-1.8}$ (95%CL) Gyr and 1.20 ± 0.06 (95%CL) $M_\odot$ (dashed line). However, as Figure 5.3 shows, a 2σ deviation (dashed error bar line) in both $T_{\rm eff}$ and $\log(L/L_\odot)$ are consistent with the 30 Myr isochrone. Based on the HR diagram, the age of HD 984 is between ZAMS (~ 30 Myr) and 4 Gyr.

5.5 Companion Characteristics

Based on the NaCo L' photometry alone, the companion mass can only be estimated from theoretical models which are highly dependent on the age of the star and lead to large uncertainties in the determined mass. Using the COND evolu-

[2] 17 November 2014 version at http://vizier.cfa.harvard.edu/viz-bin/Cat?B/wds.

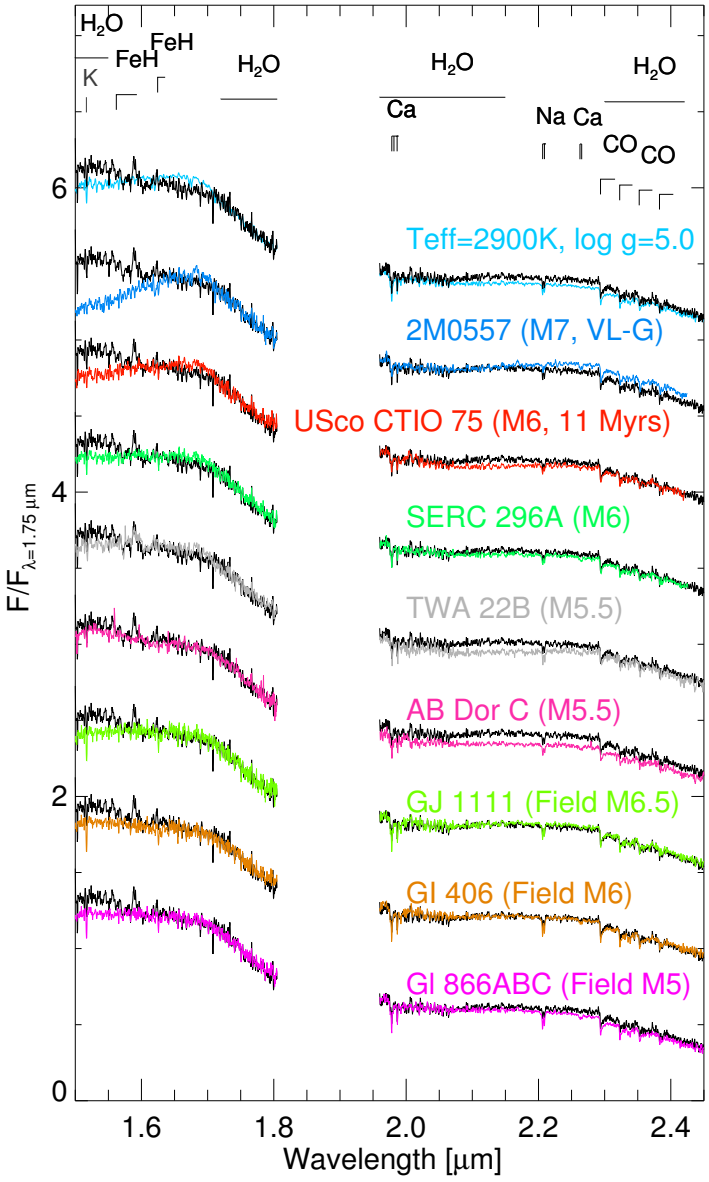

Figure 5.4 Comparison of HD 984 B spectrum (black) to those of field dwarfs, young companions, isolated objects, and to the best-fitting BT-COND spectrum. It enables us to conclude that HD 984 B is an M6.0 ± 0.5 dwarf.

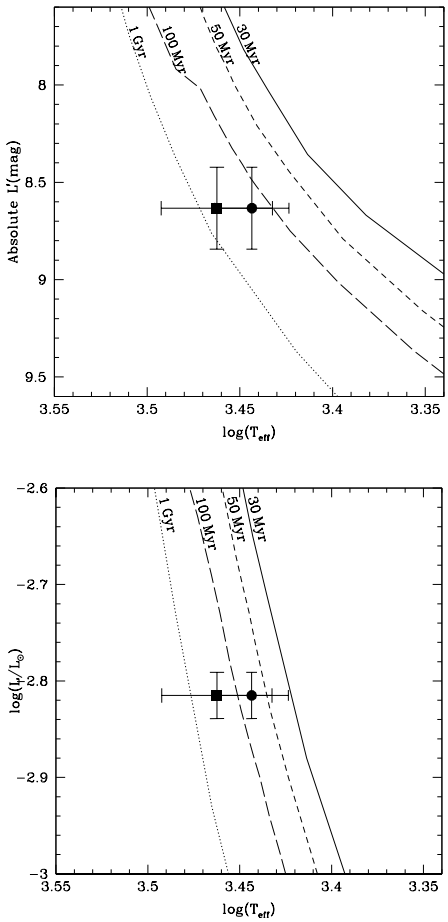

Figure 5.5 HR diagram position of HD 984 B in L'-band absolute mag (left) and bolometric luminosity (right) based on our spectral type estimate and adopting the Stephens et al. (2009) T_{eff} scale (circle), BT-COND and GAIA synthetic spectra (Brott & Hauschildt (2005); Allard et al. (2013): square). The COND evolutionary tracks (Baraffe et al. 2003) are plotted for 30, 50, 100 Myr and 1 Gyr. The >1 Gyr isochrones overlap with 1 Gyr in the COND model and thus are not shown. The companion L'-band position on the evolutionary tracks allows us to rule out an age of 50 Myr and younger. However, the companion bolometric luminosity position is nearly consistent with all evolutionary tracks, including those <50 Myr. Due to this inconsistency, the age of the system remains unconstrained.

tionary tracks (Baraffe et al. 2003), if the system is 30 Myr, the companion may be a 33 ± 6$M_{\rm Jup}$ young brown dwarf. If the system is 4 Gyr, the companion may be a $0.12 \pm 0.01 M_{\odot}$ low mass star, likely an M5-M6 dwarf. The errors are based on the uncertainty in the photometry and the distance of the star and do not include systematic uncertainties in the models. The range of companion masses based on the DUSTY evolutionary model (Chabrier et al. 2000) is within the errors of the values derived from the COND model: 30 Myr and 34 ± 6$M_{\rm Jup}$ or 4 Gyr and $0.12 \pm 0.01 M_{\odot}$. Thus, the companion mass estimation based on photometry is not significantly impacted by the evolutionary model chosen.

We compare our CADI analysis of the SINFONI spectrum (black spectrum, see Figure 5.4) with field dwarfs from the IRTF library (Rayner et al. 2009). We perform a least squares fit of the spectra to determine the best fit. In addition to the overall spectral slope from 1.5 to 2.45 μm, we aim to fit the following spectral features: the K I band at 1.516 μm, the Ca I triplet near 1.98 μm, the Na I doublet near 2.207 μm, the CO overtones longward of 2.3 μm, and the overall shape of the Ks-band which is sensitive to the collision-induced absorption of molecular hydrogen, thus to the atmospheric pressure and surface gravity. The companion has features later than M5 and midway between those of M5.5 and M6.5 field dwarfs. The SINFONI spectra of the young (≤150 Myr) mid-M companions AB Dor C and TWA 22 B (Close et al. 2007; Bonnefoy et al. 2009) reproduce the pseudo-continuum in the H-band, but have bluer slopes than our companion, suggesting a later spectral type for HD 984 B. Spectra of other young mid-M dwarfs have a more triangular H-band shape than our object. The companion fits well with the M6 object SERC 296A (Thackrah et al. 1997; Allers & Liu 2013), which does not appear to be a good candidate member to any nearby associations based on its kinematics (Gagné et al. 2014), but has an age below ~ 200 Myr due to lithium absorption. We therefore conclude that the HD 984 B is more likely a M6.0±0.5 object, which is younger than the typical field dwarf age (>>1 Gyr). The subtype accuracy is due to the companion features being intermediate between a M5.5 and an M6.5.

The spectral type of M6.0 ± 0.5 corresponds to $T_{\rm eff} = 2777^{+127}_{-130}$ K using the conversion scale of Stephens et al. (2009). The $T_{\rm eff}$ accuracy is the quadratic combination of the spectral type estimate and systematic uncertainty. Conversely, the companion's pseudo-continuum shape and main absorption features are best reproduced by BT-COND and GAIA synthetic spectra (Brott & Hauschildt 2005; Allard et al. 2013) with $T_{\rm eff} = 2900 \pm 200$ K and log g=5.0-5.5 dex. The accuracy on $T_{\rm eff}$ is limited by the intrinsic differences and uncertainties between the atmospheric model grids (H-band is known to be badly reproduced by models, see Bonnefoy et al. 2013). Rajpurohit et al. (2013) find a $T_{\rm eff}$ range of 2700 to 3000 K for M5.5 to M6.5 dwarfs by fitting BT-Settl (Allard et al. 2013) spectra to optical spectra of M-dwarfs. This is consistent with our spectral type and derived temperature.

We calculate the bolometric luminosity based on our derived spectral type and H, Ks and L'-band companion magnitude measurements. We adopt bolometric corrections of $BC_{H(B)} = 2.588 \pm 0.032$ mag, $BC_{Ks(B)} = 2.940 \pm -0.015$ mag, and $BC_{L'(B)} = 3.260 \pm 0.022$ mag by interpolating between an M6 and M7 dwarf, using

bolometric correction and color information for M dwarfs from Pecaut & Mamajek (2013), Schmidt et al. (2014), and Dupuy & Liu (2012). By taking the weighted mean of our bolometric luminosity calculations from H, Ks and L'-band measurements, we find $\log(L/L_\odot)$=-2.815±0.024 dex. These results are summarized in Table 5.1.

Figure 5.5 compares the derived T_{eff} of the companion against COND evolutionary tracks of different ages. The companion absolute L' does not fit with COND evolutionary tracks less than 50 Myr (Figure 5.5). This older age is consistent with the lack of triangular H-band shape, the surface gravity inferred from the atmospheric models, and suggests that HD 984 is a Columba interloper. However, comparing our derived bolometric luminosity with COND evolutionary tracks suggests that the companion is consistent with an age of ≥30 Myr. This discrepancy is likely due uncertainties in atmospheric models and a systematic difference in the T_{eff} scale of Stephens et al. (2009) compared with the colors from the COND model (Baraffe et al. 2003). A similar model discrepancy was shown in Mamajek et al. (2013), where the COND evolutionary tracks do not accurately predict the empirical main sequence on a color-magnitude diagram. HD 984 B demonstrates the challenges in fitting M-dwarfs on low mass evolutionary tracks. Thus, the age of the system remains unconstrained, but we have demonstrated that this companion is consistent with an M6.0 ± 0.5 object.

5.6 Conclusion

We report the discovery of a low-mass companion to the F7V star HD 984. This companion was detected in L'-band with the Apodizing Phase Plate coronagraph and non-coronagraphic photometry with the NaCo instrument on the VLT. HD 984 has been reported to be part of the 30 Myr old Columba association. However, based on our independent analysis of its HR diagram position, we estimate a main sequence isochronal age of $2.0^{+2.1}_{-1.8}$ Gyr. Due to the age uncertainty, the companion mass may range from a low mass brown dwarf (~33 M_{Jup}) to an M dwarf (~0.11 $M_\odot$), using the COND evolutionary models.

We analyze the slope and shape of SINFONI $H+K$ IFU data of the companion compared with field M dwarfs. We conclude the companion is an M6.0 ± 0.5 dwarf. Using our derived spectral type, we aim to determine the age of the system by placing the companion L'-band absolute magnitude and bolometric luminosity on COND evolutionary tracks. While the L'-band HR diagram position allows us to rule out an age less than 50 Myr, the companion's bolometric luminosity position is consistent with an age of ≥30 Myr. Thus, we cannot set age constraints on the companion, due to this discrepancy between the companion's position on evolutionary tracks.

Given its small projected separation of just ~9 AU, HD 984 B will show significant orbital motion over the next few years, allowing the potential for dynamical mass determination. In order to determine the individual mass components of the HD 984 system, RV data must be obtained. Using the current projected separation as an approximation for the semi-major axis and assuming a circular orbit, we

would expect to detect a maximum semi-amplitude from RV of 1.01 km/s for an M-dwarf companion and 0.27 km/s for a brown dwarf. This calculation assumes the orbit is edge-on (i=90°), however based on our two epoch astrometric measurements, its orbit is unlikely to be edge-on. Even if the companion is nearly face-on (i=1°), the semi-amplitude of 0.018 km/s for an M-dwarf and 0.005 km/s for a brown dwarf is within the detection limits of RV. Thus, the dynamical mass of this companion can be achieved with RV measurements and will provide a crucial comparison with the theoretical evolutionary models for mass determination.

We have demonstrated that, given the difficulty in deriving a reliable age for HD 984 that is independent of its purported group membership, the derived color and spectral parameters of the companion are necessary to determine the companion mass. These results suggest that caution should be used when estimating the masses of companions based on photometric data and stellar age based on kinematic group membership alone. It reinforces the importance of future near-infrared high contrast integral field spectrographs to the characterization of low-mass stellar and substellar companions.

Acknowledgments

TM and MAK acknowledge funding under the Marie Curie International Reintegration Grant 277116 submitted under the Call FP7-PEOPLE-2010-RG. EEM acknowledges support from NSF award AST-1313029. Part of this work has been carried out within the frame of the National Centre for Competence in Research PlanetS supported by the Swiss National Science Foundation. SPQ and MRM acknowledge the financial support of the SNSF AML, GC, and JR acknowledge financial support from the French National Research Agency (ANR) through project grant ANR10-BLANC0504-01. This letter makes use of the SIMBAD Database and the Vizier Online Data Catalog.

5.7 Appendix

We calibrated the absolute orientation of the field of view of SINFONI using observations of GQ Lup B from UT 2013 August 24 (technical program ID 60.A-9800). These observations were obtained using the pre-optics offering a 50×100 mas sampling in the $H+K$ band. During the 54 min pupil tracking (PT) sequence, 100×7s integrations were recorded. The field rotated by 12.84°. We reduced these data following the same procedure as HD 984 B. Once the cubes were corrected for atmospheric refraction, we removed the halo from the primary star centered in the field of view with a radial profile.

We found that a clockwise rotation by the $ADA.POSANG + C$ values of each data cubes re-aligned the final GQ Lup data cubes with the North. $ADA.POSANG$ is a variable found in the image header, corresponding to the position angle of the rotator at the Cassegrain focus at the time of the observations. C is an additional offset related to the calibration of the instrument rotator true North position.

We define $ROT.PT.OFF + C = 180° + ADA.PUPILPOS + C$, the angular offset needed to realign the frames to the North when the parallactic angle is 0. *ADA.PUPILPOS* is a keyword stored into the file header, which depends on the telescope pointing position and time of observation. It is redefined at the beginning of any PT sequence, but it remains constant during a PT observing sequence.

We verified that this relation remains valid for other datasets obtained in PT mode on GQ Lup during the same night, on AB Dor C (UT 2013 October 17, 60.A-9800), and on HD 984 B (UT 2014 October 10, 2014 December 3,5,8 094.C-0719), and of the astrometric binary HD 179058 AB (UT 2014 April 26, 60.A-9800). We note that we could not use the observations of the HD179058 AB to properly calibrate the instrument plate scale and absolute orientation since the binary had likely moved on its orbit since its latest independent astrometric measurement (Tokovinin et al. 2010).

For the case of GQ Lup B, the *ADA.PUPILPOS* keyword was fixed to -0.07297. Therefore, we adopted ROT.PT.OFF=179.927. We estimated a value of C=0.0 ± 0.5° comparing the resulting position angle in the derotated cubes to the position angle of the system measured from VLT/NaCo data obtained on 2012 March 3 and reported in Ginski et al. (2014). We note that this value of C assumes that the companion did not have significant orbital motion in the course of one year. This is reasonable given the available VLT/NaCo astrometry of the system recorded since 2008 (see Table 2 of Ginski et al. 2014). We also deduce from the SINFONI data of GQ Lup B that the mean square plate scale is 49.30 ± 0.14 mas/spaxel when the 50×100 mas and $H + K$ band mode of the instrument are chosen.

References

Allard, F., Homeier, D., Freytag, B., et al. 2013, Memorie della Societa Astronomica Italiana Supplementi, 24, 128
Allers, K. N., & Liu, M. C. 2013, ApJ, 772, 79
Amara, A., & Quanz, S. P. 2012, MNRAS, 427, 948
Ballering, N. P., Rieke, G. H., Su, K. Y. L., & Montiel, E. 2013, ApJ, 775, 55
Baraffe, I., Chabrier, G., Barman, T. S., Allard, F., & Hauschildt, P. H. 2003, A&A, 402, 701
Biller, B. A., Liu, M. C., Wahhaj, Z., et al. 2010, ApJL, 720, L82
Bonnefoy, M., Chauvin, G., Dumas, C., et al. 2009, A&A, 506, 799
Bonnefoy, M., Lagrange, A.-M., Boccaletti, A., et al. 2011, A&A, 528, L15
Bonnefoy, M., Boccaletti, A., Lagrange, A.-M., et al. 2013, A&A, 555, A107
Bonnet, H., Abuter, R., Baker, A., et al. 2004, The Messenger, 117, 17
Brandt, T. D., McElwain, M. W., Turner, E. L., et al. 2014, ApJ, 794, 159
Bressan, A., Marigo, P., Girardi, L., et al. 2012, MNRAS, 427, 127
Brott, I., & Hauschildt, P. H. 2005, in ESA Special Publication, Vol. 576, The Three-Dimensional Universe with Gaia, ed. C. Turon, K. S. O'Flaherty, & M. A. C. Perryman, 565
Carpenter, J. M., Bouwman, J., Mamajek, E. E., et al. 2009, ApJS, 181, 197
Casagrande, L., Schönrich, R., Asplund, M., et al. 2011, A&A, 530, A138

Chabrier, G., Baraffe, I., Allard, F., & Hauschildt, P. 2000, ApJ, 542, 464
Chauvin, G., Faherty, J., Boccaletti, A., et al. 2012, A&A, 548, A33
Chauvin, G., Vigan, A., Bonnefoy, M., et al. 2015, A&A, 573, A127
Close, L. M., Thatte, N., Nielsen, E. L., et al. 2007, ApJ, 665, 736
Cutri, R. M., Skrutskie, M. F., van Dyk, S., et al. 2003, VizieR Online Data Catalog, 2246, 0
Davies, R. I. 2007, MNRAS, 375, 1099
Dupuy, T. J., & Liu, M. C. 2012, ApJS, 201, 19
Dupuy, T. J., Liu, M. C., Leggett, S. K., et al. 2015, ArXiv e-prints
Eisenhauer, F., Abuter, R., Bickert, K., et al. 2003, in Society of Photo-Optical Instrumentation Engineers (SPIE) Conference Series, Vol. 4841, Instrument Design and Performance for Optical/Infrared Ground-based Telescopes, ed. M. Iye & A. F. M. Moorwood, 1548–1561
ESA. 1997, VizieR Online Data Catalog, 1239, 0
Gagné, J., Lafrenière, D., Doyon, R., Malo, L., & Artigau, É. 2014, ApJ, 783, 121
Ginski, C., Schmidt, T. O. B., Mugrauer, M., et al. 2014, MNRAS, 444, 2280
Holmberg, J., Nordström, B., & Andersen, J. 2009, A&A, 501, 941
Houk, N., & Swift, C. 1999, Michigan catalogue of two-dimensional spectral types for the HD Stars ; vol. 5
Kasper, M., Amico, P., Pompei, E., et al. 2009, The Messenger, 137, 8
Kenworthy, M. A., Meshkat, T., Quanz, S. P., et al. 2013, ApJ, 764, 7
Kenworthy, M. A., Quanz, S. P., Meyer, M. R., et al. 2010, in Society of Photo-Optical Instrumentation Engineers (SPIE) Conference Series, Vol. 7735, Society of Photo-Optical Instrumentation Engineers (SPIE) Conference Series
Lenzen, R., Hartung, M., Brandner, W., et al. 2003, in Society of Photo-Optical Instrumentation Engineers (SPIE) Conference Series, Vol. 4841, Society of Photo-Optical Instrumentation Engineers (SPIE) Conference Series, ed. M. Iye & A. F. M. Moorwood, 944–952
Malo, L., Doyon, R., Lafrenière, D., et al. 2013, ApJ, 762, 88
Mamajek, E. E., & Hillenbrand, L. A. 2008, ApJ, 687, 1264
Mamajek, E. E., Meyer, M. R., Hinz, P. M., et al. 2004, ApJ, 612, 496
Mamajek, E. E., Bartlett, J. L., Seifahrt, A., et al. 2013, AJ, 146, 154
Marois, C., Lafrenière, D., Doyon, R., Macintosh, B., & Nadeau, D. 2006, ApJ, 641, 556
Masana, E., Jordi, C., & Ribas, I. 2006, A&A, 450, 735
Mason, B. D., Wycoff, G. L., Hartkopf, W. I., Douglass, G. G., & Worley, C. E. 2001, AJ, 122, 3466
Meshkat, T., Bailey, V. P., Su, K. Y. L., et al. 2015, ApJ, 800, 5
Meshkat, T., Kenworthy, M. A., Quanz, S. P., & Amara, A. 2014, ApJ, 780, 17
Nielsen, E. L., Liu, M. C., Wahhaj, Z., et al. 2012, ApJ, 750, 53
Pearce, T. D., Wyatt, M. C., & Kennedy, G. M. 2015, MNRAS, 448, 3679
Pecaut, M. J., & Mamajek, E. E. 2013, ApJS, 208, 9
Quanz, S. P., Meyer, M. R., Kenworthy, M. A., et al. 2010, ApJL, 722, L49
Rajpurohit, A. S., Reylé, C., Allard, F., et al. 2013, A&A, 556, A15
Rameau, J., Chauvin, G., Lagrange, A.-M., et al. 2013, A&A, 553, A60

Rayner, J. T., Cushing, M. C., & Vacca, W. D. 2009, ApJS, 185, 289
Reggiani, M., & Meyer, M. R. 2013, A&A, 553, A124
Reis, W., Corradi, W., de Avillez, M. A., & Santos, F. P. 2011, ApJ, 734, 8
Rousset, G., Lacombe, F., Puget, P., et al. 2003, in Society of Photo-Optical Instrumentation Engineers (SPIE) Conference Series, Vol. 4839, Society of Photo-Optical Instrumentation Engineers (SPIE) Conference Series, ed. P. L. Wizinowich & D. Bonaccini, 140–149
Schlegel, D. J., Finkbeiner, D. P., & Davis, M. 1998, ApJ, 500, 525
Schmidt, S. J., West, A. A., Bochanski, J. J., Hawley, S. L., & Kielty, C. 2014, PASP, 126, 642
Schröder, C., Reiners, A., & Schmitt, J. H. M. M. 2009, A&A, 493, 1099
Stephens, D. C., Leggett, S. K., Cushing, M. C., et al. 2009, ApJ, 702, 154
Takeda, G., Ford, E. B., Sills, A., et al. 2007, ApJS, 168, 297
Thackrah, A., Jones, H., & Hawkins, M. 1997, MNRAS, 284, 507
Thies, I., Pflamm-Altenburg, J., Kroupa, P., & Marks, M. 2015, ApJ, 800, 72
Tokovinin, A., Mason, B. D., & Hartkopf, W. I. 2010, AJ, 139, 743
Torres, C. A. O., Quast, G. R., Melo, C. H. F., & Sterzik, M. F. 2008, Young Nearby Loose Associations, ed. B. Reipurth, 757
Valenti, J. A., & Fischer, D. A. 2005, ApJS, 159, 141
van Leeuwen, F. 2007, A&A, 474, 653
Wahhaj, Z., Liu, M. C., Biller, B. A., et al. 2011, ApJ, 729, 139
Wright, J. T., Marcy, G. W., Butler, R. P., & Vogt, S. S. 2004, ApJS, 152, 261
Zuckerman, B., Rhee, J. H., Song, I., & Bessell, M. S. 2011, ApJ, 732, 61